Check for updates

Cancer Science

WILEY | JCA JAPANESE CANCER ASSOCIATION

ORIGINAL ARTICLE OPEN ACCESS

Genetics, Genomics and Proteomics

Clinical and Genetic Landscape of Glioblastoma, IDH-Wildtype With *FGFR* Gene Family Alterations

Yasuhito Kegoya[1] | Yoshihiro Otani[1] | Ryo Mizuta[1] | Ryosuke Ikemachi[1] | Mako Kamiura[1] | Joji Ishida[1] | Shinichi Toyooka[2,3] | Daisuke Ennishi[2] | Shuta Tomida[2] | Shota Tanaka[1]

[1]Department of Neurological Surgery, Okayama University Graduate School of Medicine, Dentistry, and Pharmaceutical Sciences, Okayama, Japan | [2]Center for Comprehensive Genomic Medicine, Okayama University Hospital, Okayama, Japan | [3]Department of General Thoracic Surgery and Endocrinological Surgery, Okayama University Graduate School of Medicine, Dentistry, and Pharmaceutical Sciences, Okayama, Japan

Correspondence: Yoshihiro Otani (yotani@okayama-u.ac.jp)

Received: 5 October 2025 | **Revised:** 31 January 2026 | **Accepted:** 10 February 2026

Keywords: comprehensive genomic profiling | copy number alteration | FGFR | glioblastoma | single-nucleotide variant

ABSTRACT

Glioblastoma, isocitrate dehydrogenase wildtype (GBM, IDH-wt), is a highly aggressive brain tumor with a poor prognosis. Alterations in the fibroblast growth factor receptor (*FGFR*) gene family—such as *FGFR*::*TACC* fusions and *FGFR1* mutations—have emerged as potential therapeutic targets; however, their clinical and genetic features in GBM, IDH-wt remain unclear. We analyzed 1076 GBM, IDH-wt cases using comprehensive genomic profiling data from the Center for Cancer Genomics and Advanced Therapeutics (C-CAT) database in Japan. *FGFR* alterations were detected in 8.0% of patients, including *FGFR*::*TACC* fusions (3.3%) and *FGFR1* mutations (2.9%). The *FGFR*::*TACC* fusion-positive group was older at diagnosis and showed higher frequencies of *TERT* promoter mutation and *MDM2* amplification, and lower frequencies of *EGFR* amplification and *TP53* mutation, compared with the fusion-negative group. The *FGFR1* mutation-positive group was enriched for *ATRX*, *NF1*, and *PIK3CA* mutations and had significantly fewer *TERT* promoter and *PTEN* mutations, compared with the mutation-negative group. No significant differences in overall survival were observed, although both groups tended to have longer median overall survival compared with their respective negative groups. This study represents the largest genomic cohort to date of *FGFR* alterations in GBM, IDH-wt. *FGFR*::*TACC* fusion-positive and *FGFR1* mutation-positive GBMs exhibited distinct genetic profiles, highlighting the clinical relevance of molecular subclassification and providing insight for future therapeutic strategies.

1 | Introduction

Recent advances in molecular diagnostics and specific molecular targeted therapies have increased the demand for detailed analysis of brain tumors. In particular, glioblastoma (GBM), isocitrate dehydrogenase wildtype (IDH-wt) has a poor prognosis, with a median overall survival (OS) of less than 2 years despite standard treatments such as maximal safe resection, radiotherapy, chemotherapy, and tumor treating fields therapy. Therefore, the development of novel treatments is urgently required.

Fibroblast growth factor receptors (FGFRs) are transmembrane tyrosine kinase receptors that activate oncogenic signaling pathways through ligand-induced dimerization. Aberrant FGFR activation triggers downstream pathways, including

Abbreviations: C-CAT, Center for Cancer Genomics and Advanced Therapeutics; CGP, comprehensive genomic profiling; CNA, copy number alteration; CNS, central nervous system; DCR, disease control rate; DMG, diffuse midline glioma, H3K27-altered; F1T1, FGFR1::TACC1; F3T3, FGFR3::TACC3; FGFR, fibroblast growth factor receptor; GBM, glioblastoma; ICI, immune checkpoint inhibitor; IDH-wt, isocitrate dehydrogenase wildtype; IQR, interquartile range; MAPK, mitogen-activated protein kinase; ORR, overall response rate; OS, overall survival; RTK, receptor tyrosine kinase; SNV, single-nucleotide variant; STAT3, signal transducer and activator of transcription 3; TACC3, transforming acidic coiled-coil-containing protein 3; TMB, tumor mutational burden.

This is an open access article under the terms of the Creative Commons Attribution-NonCommercial-NoDerivs License, which permits use and distribution in any medium, provided the original work is properly cited, the use is non-commercial and no modifications or adaptations are made.

© 2026 The Author(s). *Cancer Science* published by John Wiley & Sons Australia, Ltd on behalf of Japanese Cancer Association.

mitogen-activated protein kinase (MAPK), thereby promoting angiogenesis, tumor cell migration, differentiation, and proliferation [1, 2]. *FGFR* alterations—both mutations and fusions—have been identified in various cancers, including gliomas [3], and are considered actionable targets.

Among these, the gene fusion of *FGFR3* and transforming acidic coiled-coil-containing protein 3 (*TACC3*) was first reported in glioblastoma [4]. The *FGFR3*::*TACC3* (*F3T3*) fusion protein is known to promote malignant transformation not only by activating the MAPK and signal transducer and activator of transcription 3 (STAT3) pathways, but also by activating mitochondrial function and impairing mitotic regulation [5–8]. Other *FGFR* gene alterations have also been reported, including *FGFR1* (N546 and K656) mutations and *FGFR1*::*TKDD* fusion in low-grade gliomas, *FGFR1*::*TACC1* (*F1T1*) fusion in extraventricular neurocytomas, and *FGFR2*::*CTNNA3* fusion in polymorphous low-grade neuroepithelial tumors [9–11]. However, comprehensive genetic analyses of glioblastomas with *FGFR* gene alterations remain limited.

In this study, we leveraged nationwide comprehensive genomic profiling data from the Center for Cancer Genomics and Advanced Therapeutics (C-CAT) database [12, 13] to examine the clinical and genetic features of GBM, IDH-wt with *FGFR* gene family alterations, in what is, to our knowledge, the largest such cohort to date.

2 | Materials and Methods

2.1 | Study Design and Patient Data Retrieval

This retrospective study was approved by the Institutional Review Board of Okayama University Hospital (2111-047). We identified patients registered in the "Central nervous system (CNS)/brain" category of the C-CAT database between June 2019 and February 2025. Clinical, diagnostic, genomic, and treatment information was retrieved for patients. Histological diagnoses were classified according to OncoTree [14]. Regarding the pathogenicity of *FGFR* gene mutations, we defined a mutation as having an evidence level F or higher according to C-CAT and being notated in the database "clinical significance" column as "pathogenic," "likely pathogenic," "oncogenic," or "likely oncogenic" (Table S1). The diagnosis of GBM, IDH-wt was based on the fifth edition of the *WHO Classification of Tumors of the Central Nervous System* [15]. Cases with "Glioblastoma" or "Gliosarcoma" in the diagnostic or histological column were included in the analysis if they were IDH-wt. Tumors registered as grade 3 or less glioma were also classified as GBM, IDH-wt if they were IDH-wt and harbored either *EGFR* amplification or *TERT* promoter mutation. Gliomas definitively diagnosed and registered differently such as diffuse midline glioma, H3K27-altered (DMG), were excluded during the search.

2.2 | Genomic Profiling Platforms and Information

Four comprehensive genomic profiling (CGP) platforms were used: FoundationOne CDx (DNA-based, 324 genes), OncoGuide NCC Oncopanel (DNA-based, 124 genes), Guardant360 CDx (DNA-based, 74 genes), and GenMineTOP (DNA-based and RNA-based, 737 genes and 455 genes, respectively). Genomic data included tumor mutational burden (TMB), genetic rearrangements, mutations (substitutions, insertions, and deletions), and copy number alterations (CNAs).

2.3 | Statistical Analysis

Continuous variables were expressed as medians (interquartile range [IQR]) and categorical variables as *n* (%). Chi-squared tests were used to compare categorical variables. When variances were assumed to be equal, *t*-tests were applied to compare continuous variables between two groups. Mann–Whitney *U*-tests were used for nonparametric comparisons of unpaired samples, and *F*-tests were performed to evaluate equality of variances. Survival probabilities were estimated using the Kaplan–Meier method, and log-rank tests were used to compare survival distributions between groups. A p value <0.05 was considered statistically significant. All analyses were performed using GraphPad Prism (Version 9.00 for Windows; GraphPad Software, La Jolla, CA, USA).

To contextualize our prevalence estimate, we performed a meta-analysis incorporating previous reports. Data from our study were combined with those from 14 previous studies and analyzed using a random-effects model [4, 7, 16–27]. Cochran's Q test and the I^2 statistic were used to assess heterogeneity; for the Q test, a p value <0.1 indicated significant heterogeneity, while I^2 values of $<25\%$, 25%–50%, 50%–75% and $>75\%$ were interpreted as low, moderate, high and very high heterogeneity, respectively.

All statistical comparisons were conducted separately for two alteration types: (1) *FGFR*::*TACC* fusion-positive vs. fusion-negative groups, (2) *FGFR1* mutation-positive vs. mutation-negative groups, and (3) *FGFR*::*TACC* fusion-positive vs. *FGFR1* mutation-positive groups. Each comparison included all eligible GBM, IDH-wt cases, regardless of the status of other *FGFR* alterations, and no patient was counted in both positive groups for the same analysis.

3 | Results

From June 2019 to February 2025, 2848 cases categorized as "CNS/brain" were registered in the C-CAT database. Among these, 1020 cases were diagnosed histologically as "Glioblastoma" or "Gliosarcoma." Sixty-five cases with *IDH1* R132 mutations and four cases with *IDH2* R172 mutations were excluded. In addition, of the 2848 "CNS/brain" cases, 655 cases were registered as "Astrocytoma," "Anaplastic astrocytoma," "Diffuse astrocytoma," "Diffuse glioma," "Glioma," or "High-grade glioma" as a histological diagnosis. To identify molecular GBM, we excluded 197 cases with *IDH1* mutations and two cases with *IDH2* mutations, and we included 53 cases with *EGFR* amplification and 108 cases with *TERT* promoter mutations (36 cases positive for both *EGFR* amplification and *TERT* promoter mutation were adjusted to avoid double counting). In total, 1076 cases were defined as GBM, IDH-wt and subjected

13497006, 0, Downloaded from https://onlinelibrary.wiley.com/doi/10.1111/cas.70347 by Okayama University, Wiley Online Library on [13/03/2026]. See the Terms and Conditions (https://onlinelibrary.wiley.com/terms-and-conditions) on Wiley Online Library for rules of use; OA articles are governed by the applicable Creative Commons License

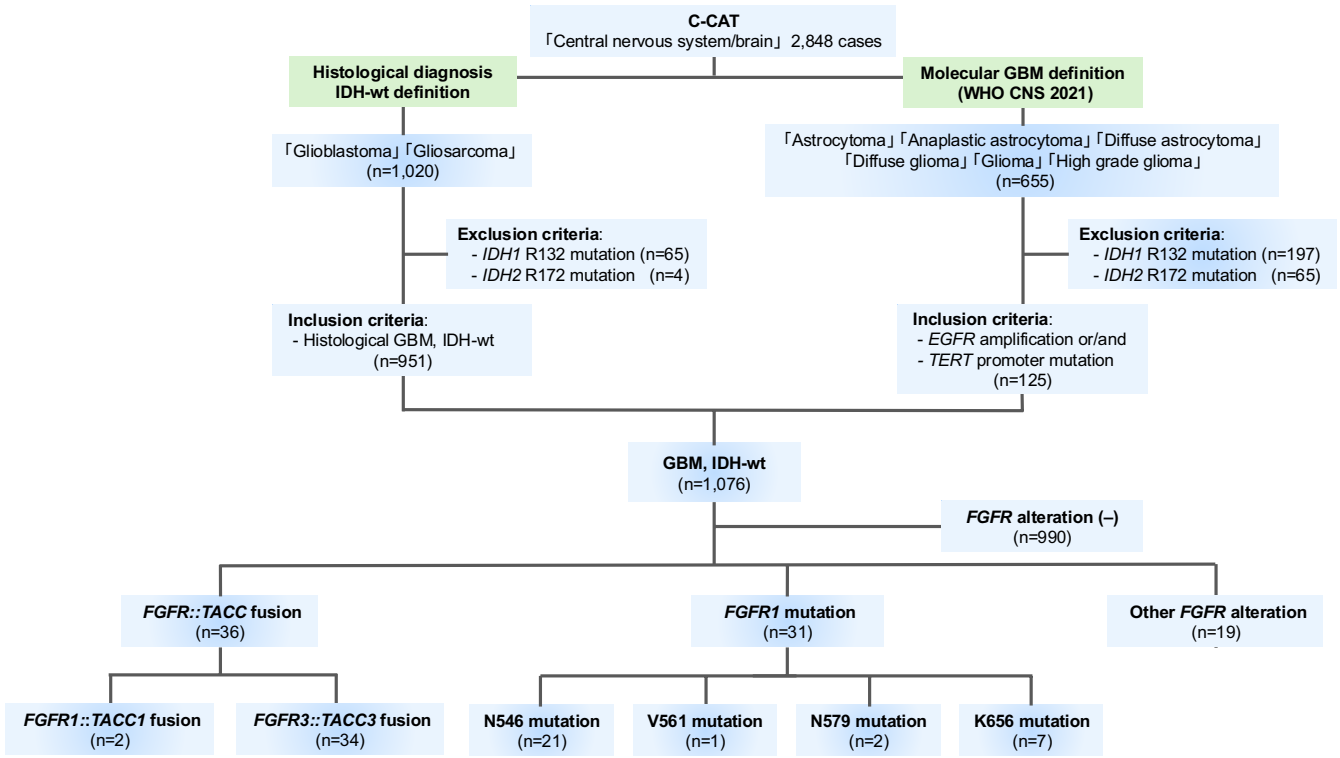

FIGURE 1 | Flowchart showing the process of selecting cases of glioblastoma, IDH-wildtype with *FGFR*::*TACC* fusion and *FGFR1* mutation in this study. This study included 2848 cases registered in the "Central Nervous System/Brain" category of the C-CAT database. In addition to cases histologically diagnosed as glioblastoma or gliosarcoma, IDH-wildtype glioma cases with either *EGFR* amplification or *TERT* promoter mutation were also included to encompass molecular glioblastoma. In total, 1076 glioblastoma, IDH-wildtype cases were included in the analysis, with 36 cases harboring *FGFR*::*TACC* fusions and 31 cases harboring *FGFR1* mutations. Other *FGFR* alterations were also present in 19 cases.

to further analysis (Figure 1). The distribution of CGP platforms among patients with GBM, IDH-wt was as follows: 76.6% (824/1076) FoundationOne CDx, 5.1% (55/1076) OncoGuide NCC Oncopanel, 0.2% (2/1076) Guardant360 CDx, and 18.1% (195/1076) GenMineTOP.

The patients' demographic data are summarized in Table 1. Of the 1076 patients, 583 (54.2%) were male, and the median age was 55 years (IQR 44–65 years). The median TMB score was 2.5 (IQR 1.1–4.3). The median number of gene rearrangements/structural atypia was 0 (IQR 0–0), and the median number of mutations including substitutions, insertions, and deletions was 6 (IQR 0–10). The median number of CNAs was 1 (IQR 0–3) (Table 1). A total of 86 patients (8.0%) harbored *FGFR* gene family alterations. *FGFR*::*TACC* fusions were detected in 36 cases (two cases with *F1T1* fusion and 34 cases with *F3T3* fusion), *FGFR1* mutation in 31 cases (21 cases with the N546 mutation, one with the V561 mutation, two with the N579 mutation, and seven with the K656 mutation), *FGFR3* amplification in 13 cases, *FGFR1* rearrangements in two cases, *FGFR3* rearrangements in two cases, and *FGFR3* K650E mutations in two cases. Additionally, *FGFR2* amplification, *FGFR2* K659 mutation, *FGFR2* R203H mutation, *FGFR3*::*STARD9* fusion, *FGFR4* amplification, and *FGFR4* loss were each observed in one case. Six patients had both *F3T3* fusion and *FGFR3* amplification (Figure 1, Figure S1, Table S2).

Kaplan–Meier analysis of OS demonstrated no significant difference between patients harboring *FGFR* gene family alterations and those without such alterations ($p = 0.568$) (Figure S2). The median OS was 31.0 months in the alteration-positive group compared with 23.1 months in the alteration-negative group.

3.1 | Clinical and Genetic Features of Glioblastoma, IDH-wt With *FGFR*::*TACC* Fusion

In the *FGFR*::*TACC* fusion-positive group, 20 of 36 cases (55.6%) were male, compared with 563 of 1040 cases (54.1%) in the fusion-negative group ($p = 0.866$). The median age was significantly higher in the fusion-positive group (60 years, IQR 52.8–66.3) than in the fusion-negative group (55 years, IQR 43.8–65) ($p = 0.012$; Table 1). Figure S3 shows violin plots comparing TMB score, the number of gene rearrangements/structural atypia, substitutions, insertions, deletions and CNAs between the *FGFR*::*TACC* fusion-positive group and the fusion-negative group (Figure S3). The median TMB score was 2 (IQR 1.1–3.8) in the fusion-positive group and 2.5 (IQR 1.1–4.3) in the fusion-negative group ($p = 0.234$). The median number of gene rearrangements/structural atypia was zero in both groups (fusion-positive: IQR 0–1; fusion-negative: IQR 0–0, $p = 0.018$). The median number of substitutions, insertions, and deletions was four in the fusion-positive group and six in the negative group (fusion-positive: IQR 0–8; fusion-negative: IQR 0–10, $p = 0.229$). The median number of CNAs was zero in the fusion-positive group and one in the fusion-negative group (fusion-positive: IQR 0–1.3; fusion-negative: IQR 0–3, $p = 0.014$) (Table 1, Figure S3). Overall, the *FGFR*::*TACC* fusion-positive group was

13497006, 0, Downloaded from https://onlinelibrary.wiley.com/doi/10.1111/cas.70347 by Okayama University, Wiley Online Library on [13/03/2026]. See the Terms and Conditions (https://onlinelibrary.wiley.com/terms-and-conditions) on Wiley Online Library for rules of use; OA articles are governed by the applicable Creative Commons License

TABLE 1 | Clinical and genetic characteristics of glioblastoma, IDH wild-type with *FGFR*::*TACC* fusion and *FGFR1* mutation.

Variable	Overall ($n=1076$)	*FGFR*::*TACC* fusion (+) ($n=36$)	*FGFR*::*TACC* fusion (−) ($n=1040$)	*p*	*FGFR 1* mutation (+) ($n=31$)	*FGFR 1* mutation (−) ($n=1045$)	*p*
Age at diagnosis							
Median [year, IQR]	55 [44–65]	60 [52.8–66.3]	55 [43.8–65]	0.012	52 [45–59.5]	55 [44–65]	0.385
Average	52.8	59.2	52.6		51.9	52.8	
Sex							
Male	583 (54.2%)	20 (55.6%)	563 (54.1%)	0.866	14 (45.2%)	569 (54.4%)	0.306
Female							
Tumor mutation burden score							
Median [number, IQR]	2.5 [1.1–4.3]	2 [1.1–3.8]	2.5 [1.1–4.3]	0.234	5 [2.4–7]	2.3 [1.1–4]	<0.001
Average	8.2	2.3	8.4		14.9	8.0	
Number of gene rearrangements/structural atypia							
Median [number, IQR]	0 [0–0]	0 [0–1]	0 [0–0]	0.018	0 [0–0]	0 [0–0]	0.016
Average	0.5	0.5	0.5		0.1	0.5	
Number of substitutions, insertions, and deletions							
Median [number, IQR]	6 [0–10]	4 [0–8]	6 [0–10]	0.229	8 [0–12]	6 [0–10]	0.090
Average	8.4	4.8	8.6		16.8	8.2	
Number of copy number alterations							
Median [number, IQR]	1 [0–3]	0 [0–1.3]	1 [0–3]	0.014	0 [0–2]	1 [0–3]	0.038
Average	2.0	0.9	2.1		1.3	2.1	

Note: For comparing categorical variables, the chi-square test was used, while the *t*-test was used for comparing continuous variables. For non-parametric tests between independent samples, the Mann–Whitney *U*-test was used. A *p* value <0.05 is considered statistically significant.

significantly older and exhibited fewer gene rearrangements/structural atypia and CNAs than the fusion-negative group.

CNA analysis of GBM, IDH-wt with *FGFR*::*TACC* fusion revealed that the frequencies of *MDM2* amplification (9/36 cases [25%], $p<0.001$) and *FGFR3* amplification (6/36 cases [16.7%], $p<0.001$) were significantly higher in the fusion-positive group. *CDK4* amplification was observed in 8/36 cases (22.2%), but was not statistically significant ($p=0.108$). In contrast, *EGFR* amplification, which was significantly more common in the fusion-negative group (316/1040 cases [30.4%], $p<0.001$), was not observed in the fusion-positive group. *KIT* amplification (99/1040 cases [9.5%], $p=0.052$) and *PDGFRA* amplification (134/1040 cases [12.9%], $p=0.106$) also tended to be more frequent in the fusion-negative group. Loss of *CDKN2B* was significantly more frequent in the fusion-negative group (395/1040 cases [38.0%], $p=0.003$) (Figure 2, Table 2).

Analysis of single-nucleotide variants (SNVs) showed that the frequency of *TERT* promoter mutations was significantly higher in the fusion-positive group than in the fusion-negative group (30/36 cases [83.3%], $p=0.004$). Conversely, *EGFR* mutations were not detected in the fusion-positive group, whereas they were significantly more frequent in the fusion-negative group (227/1040 cases [21.8%], $p=0.002$). *TP53* mutations (410/1040 cases [39.4%], $p<0.001$) and *ATM* mutations (108/1040 cases [10.4%], $p=0.042$) were also significantly more common in the fusion-negative group (Table 3).

Kaplan–Meier analysis of OS revealed no significant difference between the fusion-positive and fusion-negative groups ($p=0.171$) (Figure 3A). The median OS was 42.7 months in the fusion-positive group and 29.1 months in the fusion-negative group.

The prevalence of *F3T3* fusion-positive GBM, IDH-wt in this cohort was 3.2% (34/1076). A meta-analysis using a random-effects model, incorporating data from previous reports [4, 7, 16–27], yielded an overall prevalence of 3.1% (95% CI 2.53–3.89) (Figure 4).

13497006, 0, Downloaded from https://onlinelibrary.wiley.com/doi/10.1111/cas.70347 by Okayama University, Wiley Online Library on [13/03/2026]. See the Terms and Conditions (https://onlinelibrary.wiley.com/terms-and-conditions) on Wiley Online Library for rules of use; OA articles are governed by the applicable Creative Commons License

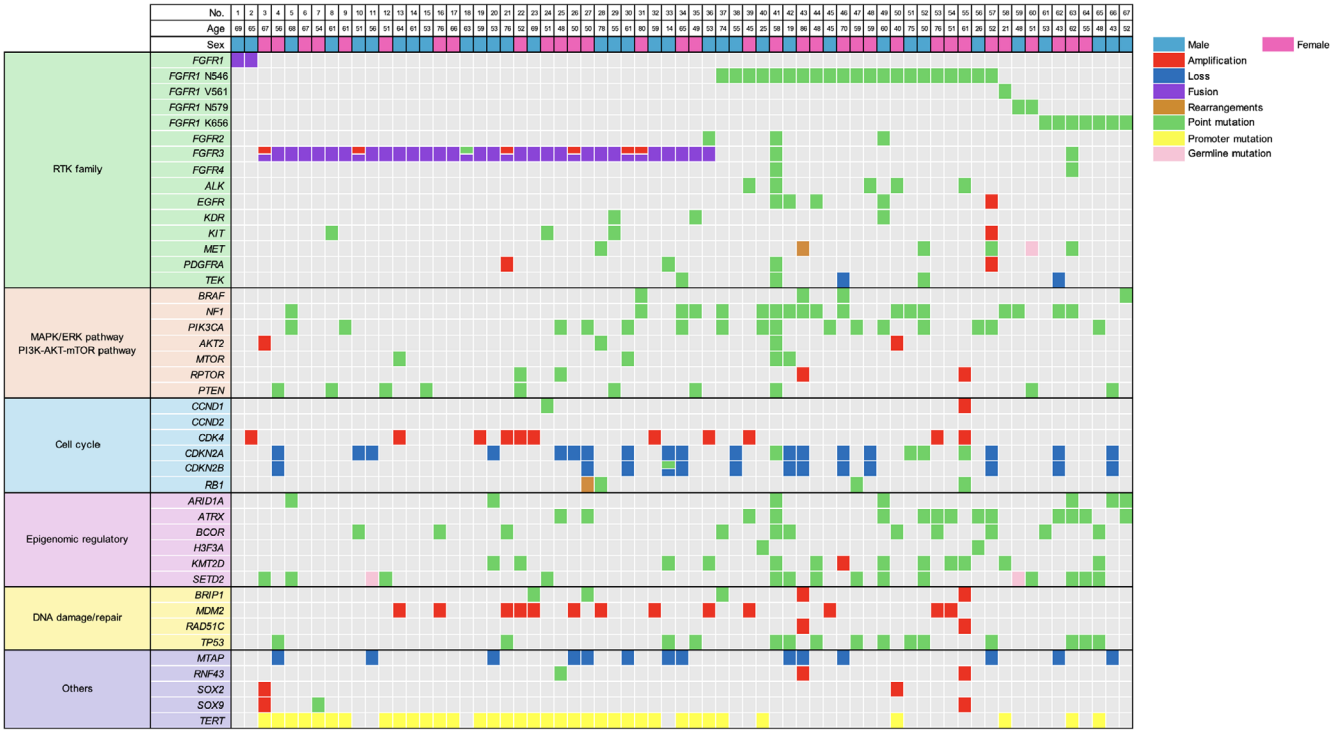

FIGURE 2 | Summary of the clinical and genetic features in patients with *FGFR*::*TACC* fusion and *FGFR1* mutation in glioblastoma, IDH-wildtype. Age, sex, and representative gene mutations are plotted for a total of 67 cases.

3.2 | Clinical and Genetic Features of Glioblastoma, IDH-wt With *FGFR1* Mutations

Among patients with GBM, IDH-wt harboring *FGFR1* mutations (mutation-positive group), 14 of 31 cases (45.2%) were male, compared with 569 of 1045 cases (54.4%) in the patients without *FGFR1* mutations (mutation-negative group) ($p = 0.306$). The median age was 52 years (IQR 45–59.5 years) in the mutation-positive group and 55 years (IQR 44–65 years) in the mutation-negative group ($p = 0.385$) (Table 1). The median TMB score was significantly higher in the mutation-positive group (5, IQR 2.4–7) compared with the mutation-negative group (2.3, IQR 1.1–4, $p < 0.001$). The median number of gene rearrangements/structural atypia was zero in both groups (both groups: IQR 0–0, $p = 0.016$). The median number of substitutions, insertions, and deletions was eight in the mutation-positive group and six in the mutation-negative group (mutation-positive: IQR 0–12, mutation-negative: IQR 0–10, $p = 0.090$). The median number of CNAs was zero in the mutation-positive group and one in the mutation-negative group (mutation-positive: IQR 0–2, mutation-negative: IQR 0–3, $p = 0.038$) (Table 1, Figure S4).

CNA analysis according to *FGFR1* mutation status showed that *BRIP1* (2/31 cases [6.5%], $p = 0.015$) and *RAD51C* (2/31 cases [6.5%], $p = 0.027$) amplifications were significantly more frequent in the mutation-positive group (Figure 2, Table 2). By contrast, *EGFR* amplification was significantly more common in the mutation-negative group (315/1045 cases [30.1%], $p < 0.001$), with only one case in the mutation-positive group. *CDKN2A* loss also tended to be more frequent in the mutation-negative group (433/1045 cases [41.4%], $p = 0.081$) (Figure 2, Table 2).

As a result of analyzing SNVs between the *FGFR1* mutation-positive and mutation-negative groups, the frequencies of SNVs in *NF1* (14/31 cases [45.2%], $p < 0.001$), *ATRX* (12/31 cases [38.7%], $p < 0.001$), *PIK3CA* (10/31 cases [32.3%], $p = 0.001$), *SETD2* (10/31 cases [32.3%], $p < 0.001$), *BCOR* (8/31 cases [25.8%], $p < 0.001$), *KMT2D* (8/31 cases [25.8%], $p = 0.020$), *PTPN11* (6/31 cases [19.4%], $p = 0.002$), *ALK* (5/31 cases [16.1%], $p < 0.001$), *ARID1A* (5/31 cases [16.1%], $p = 0.042$), *KMT2A* (5/31 cases [16.1%], $p = 0.021$), and *PIK3C2G* (5/31 cases [16.1%], $p = 0.009$) genes were significantly higher in the *FGFR1* mutation-positive group (Table 3, Table S3). In contrast, *TERT* promoter mutations were detected in only six cases, in the mutation-positive group, but were significantly more common in the mutation-negative group (641/1045 cases [61.3%], $p < 0.001$). *PTEN* mutations (326/1045 cases [31.2%], $p = 0.010$) were also significantly more frequent in the mutation-negative group (Table 3). Table 4 summarizes details of *ATRX*, *NF1*, *PIK3CA*, and *SETD2* mutations, which were significantly more frequent in the *FGFR1* mutation-positive group. All point mutations in these four genes (*ATRX*: 12/12 cases, *NF1*: 14/14 cases, *PIK3CA*: 10/10 cases, *SETD2*: 10/10 cases) were classified as clinically significant variants (Table 4).

A Kaplan–Meier analysis comparing OS between the mutation-positive and mutation-negative groups showed no significant difference ($p = 0.795$) (Figure 3B). The median OS was 40.8 months in the mutation-positive group and 30.3 months in the mutation-negative group.

13497006, 0, Downloaded from https://onlinelibrary.wiley.com/doi/10.1111/cas.70347 by Okayama University, Wiley Online Library on [13/03/2026]. See the Terms and Conditions (https://onlinelibrary.wiley.com/terms-and-conditions) on Wiley Online Library for rules of use; OA articles are governed by the applicable Creative Commons License

TABLE 2 | Comparison of copy number alteration frequencies in *FGFR*::*TACC* fusion and *FGFR1* mutation subgroups of glioblastoma, IDH-wildtype, ordered by overall alterations frequency.

Variable	Overall ($n=1076$)	*FGFR*::*TACC* fusion (+) ($n=36$)	*FGFR*::*TACC* fusion (−) ($n=1040$)	*p*	*FGFR1* mutation (+) ($n=31$)	*FGFR1* mutation (−) ($n=1045$)	*p*
Amplification							
EGFR	316	0	316	<0.001	1	315	0.001
CDK4	143	8	135	0.108	3	140	0.548
PDGFRA	135	1	134	0.106	1	134	0.112
KIT	99	0	99	0.052	1	98	0.243
MDM2	81	9	72	<0.001	4	77	0.250
KDR	72	0	72	0.102	0	72	0.130
MDM4	44	0	44	0.208	0	44	0.243
PIK3C2B	43	0	44	0.213	0	43	0.249
MET	38	0	38	0.243	0	38	0.280
SOX2	37	1	36	0.825	1	36	0.947
CDK6	24	0	24	0.357	0	24	0.393
HGF	20	1	19	0.678	0	20	0.437
IKZF1	18	0	18	0.426	0	18	0.461
RAD51C	17	0	17	0.439	2	15	0.027
RNF43	17	0	17	0.439	1	16	0.456
BRIP1	15	0	15	0.468	2	13	0.015
CCND2	13	0	13	0.500	0	13	0.532
FGFR3	13	6	7	<0.001	0	13	0.532
MYC	13	1	12	0.381	0	13	0.532
GRM3	12	0	12	0.517	0	12	0.549
MYCN	12	0	12	0.517	0	12	0.549
SOX9	12	1	11	0.334	1	11	0.256
Loss							
CDKN2A	441	10	431	0.101	8	433	0.081
CDKN2B	400	5	395	0.003	8	392	0.184
MTAP	304	8	296	0.414	5	299	0.128
PTEN	58	0	58	0.145	0	58	0.177
TEK	29	0	29	0.310	2	27	0.190
NF1	17	0	17	0.439	0	17	0.474
FAS	16	0	16	0.453	0	16	0.488
ERRFI1	15	0	15	0.468	0	15	0.502
CDKN2C	15	0	15	0.468	0	15	0.502
RB1	14	0	14	0.483	0	14	0.517
TP53	8	0	8	0.597	0	8	0.625

Note: A chi-square test was used to determine statistical significance. A p value <0.05 is considered statistically significant.

13497006, 0, Downloaded from https://onlinelibrary.wiley.com/doi/10.1111/cas.70347 by Okayama University, Wiley Online Library on [13/03/2026]. See the Terms and Conditions (https://onlinelibrary.wiley.com/terms-and-conditions) on Wiley Online Library for rules of use; OA articles are governed by the applicable Creative Commons License

TABLE 3 | Comparison of single-nucleotide variant frequencies in *FGFR*::*TACC* fusion and *FGFR1* mutation subgroups of glioblastoma, IDH-wildtype, ordered by overall mutation frequency.

Variable	Overall ($n=1076$)	*FGFR*::*TACC* fusion (+) ($n=36$)	*FGFR*::*TACC* fusion (−) ($n=1040$)	*p*	*FGFR1* mutation (+) ($n=31$)	*FGFR1* mutation (−) ($n=1045$)	*p*
TERT promoter	647	30	617	0.004	6	641	< 0.001
TP53	414	4	410	< 0.001	11	403	0.728
PTEN	329	7	322	0.140	3	326	0.010
NF1	233	4	229	0.118	14	219	0.001
EGFR	227	0	227	0.002	4	223	0.257
NOTCH3	160	4	156	0.519	6	154	0.476
PIK3CA	141	6	135	0.519	10	131	0.001
KMT2D	132	4	128	0.830	8	124	0.020
SETD2	131	4	127	0.843	10	121	< 0.001
NOTCH1	129	5	124	0.721	4	125	0.874
PDGFRA	125	1	124	0.092	1	124	0.139
SPEN	112	2	110	0.332	2	110	0.464
RB1	111	1	110	0.130	2	109	0.473
ATRX	109	2	107	0.355	12	97	< 0.001
ATM	108	0	108	0.042	5	103	0.252
LTK	104	4	100	0.765	5	99	0.217
ROS1	103	4	99	0.750	2	101	0.549
BRAF	95	1	94	0.193	3	92	0.866
BRCA2	92	2	90	0.513	5	87	0.126
STK11	91	2	89	0.524	0	91	0.086
TSC2	91	0	91	0.064	4	87	0.367
PIK3R1	90	2	88	0.536	5	85	0.113
FANCA	80	3	77	0.834	4	76	0.239
KEL	80	3	77	0.834	0	80	0.109
TSC1	77	1	76	0.300	3	74	0.581
MTOR	77	2	75	0.705	2	75	0.877
BCOR	77	4	73	0.349	8	69	< 0.001
CIC	76	3	73	0.762	2	74	0.893
ARID1A	75	2	73	0.735	5	70	0.042
MSH6	74	3	71	0.725	3	71	0.532
APC	72	2	70	0.781	2	70	0.957
BCORL1	68	0	68	0.114	4	64	0.126
CREBBP	68	0	68	0.113	4	64	0.126
POLE	68	3	65	0.614	4	64	0.126
PTPN11	68	0	68	0.114	6	62	0.002

Note: A chi-square test was used to determine statistical significance. A p value < 0.05 is considered statistically significant.

13497006, 0, Downloaded from https://onlinelibrary.wiley.com/doi/10.1111/cas.70347 by Okayama University, Wiley Online Library on [13/03/2026]. See the Terms and Conditions (https://onlinelibrary.wiley.com/terms-and-conditions) on Wiley Online Library for rules of use; OA articles are governed by the applicable Creative Commons License

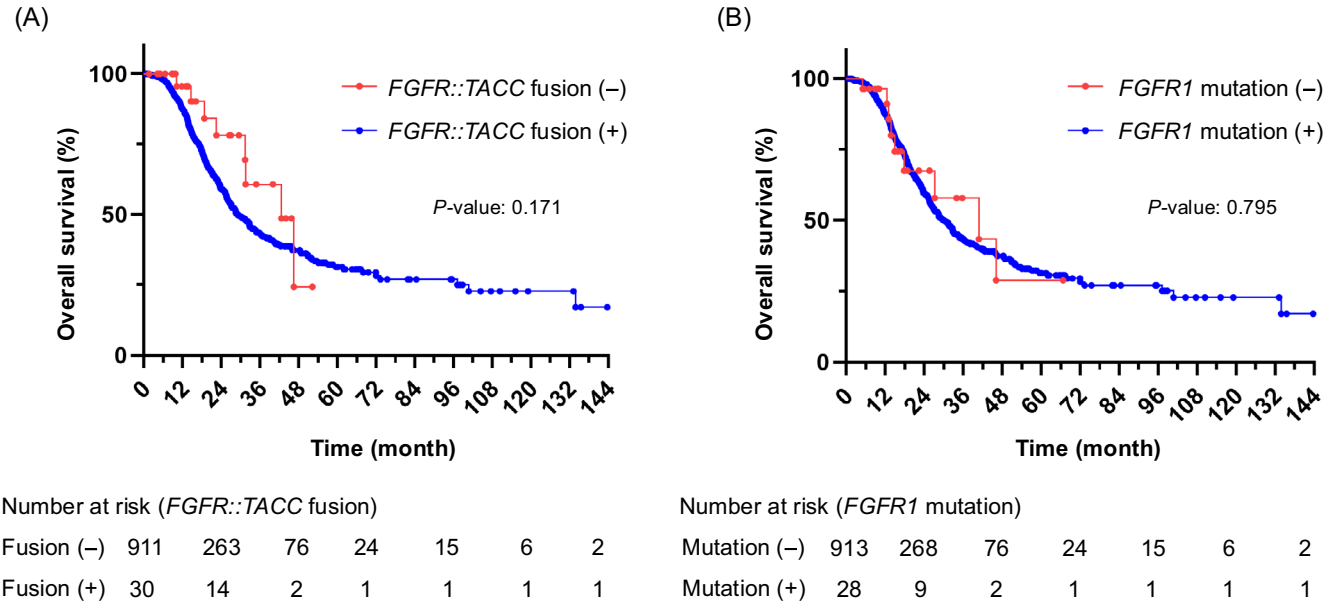

Number at risk (*FGFR::TACC* fusion)

Fusion (–)	911	263	76	24	15	6	2
Fusion (+)	30	14	2	1	1	1	1

Number at risk (*FGFR1* mutation)

Mutation (–)	913	268	76	24	15	6	2
Mutation (+)	28	9	2	1	1	1	1

FIGURE 3 | Kaplan–Meier survival curve demonstrating overall survival. (A) *FGFR::TACC* fusion-positive vs. fusion-negative, (B) *FGFR1* mutation-positive vs. mutation-negative. The number at risk was listed every 24 months. Statistical significance was assessed by the log-rank test, with $p < 0.05$ considered significant.

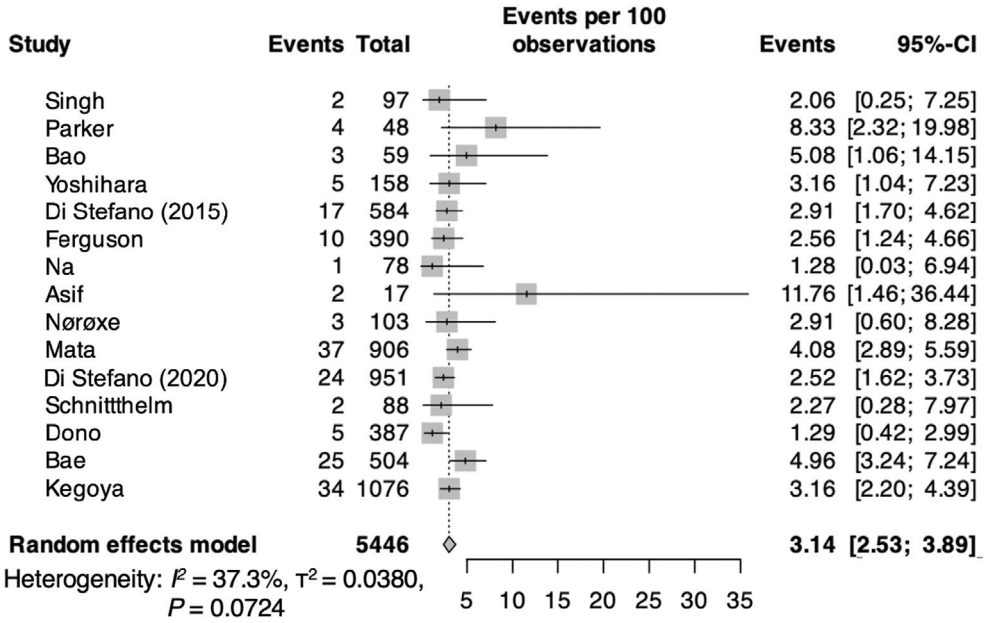

FIGURE 4 | Prevalence of *FGFR3::TACC3* fusion-positive glioblastoma, IDH-wildtype. The results of this study were analyzed using a random effects model, along with data from 14 previously published studies.

3.3 | Comparison of Clinical and Genetic Characteristics of Glioblastoma, IDH-wt With *FGFR::TACC* Fusion and Those With *FGFR1* Mutations

Comparing the clinical and genetic characteristics of *FGFR::TACC* fusion-positive and *FGFR1* mutation-positive GBM, IDH-wt, we found that the former group was significantly older and exhibited significantly more gene rearrangements/structural atypia than the latter (Table S4). Kaplan–Meier analysis of OS between the groups revealed no significant difference ($p = 0.435$) (Figure S5).

4 | Discussion

The current study represents the largest one to date elucidating the clinical and genetic characteristics of GBM, IDH-wt with *FGFR* family alterations. Recent genetic studies have identified *FGFR* alterations—including fusion genes and point mutations—in approximately 3% of infiltrating gliomas [26] making them promising therapeutic targets. In the RAGNAR study [28] (NCT04083976), erdafitinib, an oral, selective pan-FGFR tyrosine kinase inhibitor, achieved an overall response rate (ORR) of 13.5% and disease control rate (DCR) of 59.5% among glioma patients, with higher activity in low-grade

13497006, 0, Downloaded from https://onlinelibrary.wiley.com/doi/10.1111/cas.70347 by Okayama University, Wiley Online Library on [13/03/2026]. See the Terms and Conditions (https://onlinelibrary.wiley.com/terms-and-conditions) on Wiley Online Library for rules of use; OA articles are governed by the applicable Creative Commons License

TABLE 4 | Details of representative genes (*ATRX*, *NF1*, *PIK3CA*, *SETD2*) that were significantly more prevalent in the *FGFR1*-positive group.

Variable	Age	Sex	*FGFR1*	*ATRX*	*NF1*	*PIK3CA*	*SETD2*	Other alterations
Case 37	74	M	N546K	—	c.1527+1G>T	H1047R	—	*TERT* c.-79-45C>T
Case 38	55	M	N546K	—	—	—	—	*CDKN2A/B* loss
Case 39	45	F	N546K	L464fs*4	—	—	—	*CDK4* amplification, *MDM2* amplification
Case 40	25	M	N546K	—	R192*	P104L	E542K	*TERT* c.-79-45C>T, *H3F3A* K28M
Case 41	58	F	N546D	T1749I	G57D, L2007P, C93fs*14, T990fs*2, R1653H	R88Q, Q546H	G1434E, L716F, V779F, R520fs*59	*BCOR* R1480*, *CDKN2A* P114L, P114S *PDGFRA* D1071N, *PTEN* R233Q *TP53* R196*
Case 42	19	M	N546K	—	R1968*, I679fs*21	—	R540*, R136T	*CDKN2A/B* loss, *EGFR* A289V *TP53* Q317fs*28, R273C
Case 43	86	F	N546K	—	W426*	—	—	*CDKN2A/B* loss
Case 44	48	F	N546K	—	G311V	—	E251Q	*TP53* R282W
Case 45	45	M	N546K	—		E542K	—	*MDM2* amplification
Case 46	70	F	N546K	—	Y1608S	—	—	*CDKN2A/B* loss
Case 47	59	F	N546D	—	—	R88Q	G1563D	*TP53* R273C
Case 48	59	F	N546K	—	—	—	—	*CDKN2A/B* loss
Case 49	60	M	N546K	R1302fs*44	—	H1047R	D2064fs*8, M1526V	*TP53* P301fs*44, R273H
Case 50	40	F	N546K	—	c.7063-1delG, I2003fs*9	—	—	*AKT2* amplification, *SOX2* amplification *TERT* c.-79-45C>T
Case 51	75	M	N546K	—	R1534*	—	—	*CDKN2A* R58*, *TP53* R213Q
Case 52	50	M	N546K	R1743del	I603K	C407R, R88Q	Q1301*, R2121H	—
Case 53	76	F	N546K	S282N	—	—	—	*CDK4* amplification, *MDM2* amplification
Case 54	51	F	N546K	S559*	—	—	—	*MDM2* amplification
Case 55	61	F	N546K	—	—	—	—	*CCND1* amplification, *FGF19* amplification *CDK4* amplification *CDKN2A* c.151-18_152del20
Case 56	26	M	N546K	S576fs*4	—	D454N, E453K	—	—

(Continues)

13497006, 0, Downloaded from https://onlinelibrary.wiley.com/doi/10.1111/cas.70347 by Okayama University, Wiley Online Library on [13/03/2026]. See the Terms and Conditions (https://onlinelibrary.wiley.com/terms-and-conditions) on Wiley Online Library for rules of use; OA articles are governed by the applicable Creative Commons License

TABLE 4 | (Continued)

Variable	Age	Sex	*FGFR1*	*ATRX*	*NF1*	*PIK3CA*	*SETD2*	Other alterations
Case 57	52	F	N546K	S1245fs*1	—	H1047R	—	*CDKN2A/B* loss, *EGFR* amplification *KIT* amplification, *PDGFRA* amplification
Case 58	21	F	V561M	—	E688*, V141fs*24	—	—	*TERT* c.-79-45C>T
Case 59	48	M	N579K	—	R2258*	—	—	—
Case 60	51	F	N579K	—	—	—	V1656F	—
Case 61	53	M	K656E	—	—	—	—	*BCOR* A230fs*31
Case 62	43	F	K656E	c.6217+1_6217+2insA	P1604_Y1607del, W2712*	—	—	*CDKN2A/B* loss
Case 63	62	F	K656E	T1582fs*19	Y2485fs*2	—	c.70_71+2delGAGT, R540*	*TERT* c.-79-24C>T *TP53* G245S
Case 64	55	F	K656E	V2037F	—	—	R329Q, S725del	*TP53* P278S
Case 65	48	M	K656E	—	—	E545K	R1625H, E972K	*BCOR* E1042fs*26 *TERT* c.-79-45C>T *TP53* R342*, Y163D
Case 66	43	M	K656E	—	—	—	—	*CDKN2A/B* loss, *PTEN* I135V
Case 67	52	M	K656E	T1404fs*96	—	—	—	—

Note: Those with evidence level *F* or higher (known to be involved in tumorigenesis) in the C-CAT database are listed.

13497006, 0, Downloaded from https://onlinelibrary.wiley.com/doi/10.1111/cas.70347 by Okayama University, Wiley Online Library on [13/03/2026]. See the Terms and Conditions (https://onlinelibrary.wiley.com/terms-and-conditions) on Wiley Online Library for rules of use; OA articles are governed by the applicable Creative Commons License

gliomas (ORR 29%, DCR 71%) than in high-grade gliomas (ORR 10%, DCR 57%). In the TARGET study (NCT02824133) [29], fexagratinib was administered to patients with relapsed or refractory *FGFR* fusion-positive gliomas and demonstrated acceptable toxicity. These studies highlighted the importance of comprehensively understanding the prevalence of *FGFR* alteration in GBM, IDH-wt, and the genetic features of *FGFR* altered GBM, IDH-wt.

4.1 | *FGFR*::*TACC* Fusion in GBM, IDH-wt

Among the FGFR family (FGFR1–FGFR4), gene fusions with FGFR1 and FGFR3 often occur due to small chromosomal deletions, resulting in fusions with nearby partner genes. In contrast, FGFR2 frequently translocates to partners on other chromosomes. Among these alterations, *F3T3* fusion and *FGFR3* amplification are the most common *FGFR* alterations in adult IDH-wt infiltrating gliomas. According to a previous systematic review [23], approximately 3% of GBMs harbor the *F3T3* fusion. In our analysis, the prevalence of *F3T3* fusion in GBM, IDH-wt was consistent with pooled estimates from previous studies, supporting external validity [4, 7, 16–27] (Figure 4). We also identified two cases of *F1T1* fusion-positive GBM, IDH-wt. *F1T1* fusions are usually observed in extraventricular neurocytomas and are typically confined to low-grade tumors; to our knowledge, there have been no prior reports of *F1T1* fusion in GBM, IDH-wt [6, 30].

Recent genetic and epigenetic studies have identified GBM, IDH-wt harboring *F3T3* fusion as a distinct subtype associated with improved survival [23, 31, 32]. Mata et al. reported that *F3T3* fusion-positive GBMs were predominantly classified as GBM-mesenchymal and receptor tyrosine kinase (RTK)-II subclasses, and that patients survived approximately 8 months longer than fusion-negative patients [23]. Furthermore, van der Meulen et al. reported that GBM patients who survived more than 5 years had a higher prevalence of *F3T3* fusion [32]. Di Stefano et al. also reported improved survival in *F3T3* fusion-positive GBM (median OS: 31.1 months), with *F3T3* fusion being an independent predictor of better survival in multivariate analysis [24]. In our study, we were unable to demonstrate that the presence of *F3T3* fusion contributed to prolonged OS. A limitation of the C-CAT data is the selection bias due to left truncation, meaning that cases with a markedly poor prognosis could not be registered [33]. In Japan, insurance restrictions delay CGP until late in the disease course, potentially excluding patients with rapid progression. This may attenuate observed survival differences.

Regarding genetic features, recent studies have shown that patients with *F3T3* fusion harbor mutually exclusive amplifications of *EGFR*, *PDGFRA*, and *MET*; frequent amplifications of *CDK4* and *MDM2*; frequent co-mutations of the *TERT* promoter; and rare oncogenic changes in *TP53* [1, 7, 18, 23, 34, 35]. In this study, consistent with previous reports, *MDM2* amplification was significantly more common in the *FGFR*::*TACC* fusion-positive group, whereas *EGFR* amplification was significantly less frequent. The frequencies of *CDK4* amplification tended to be higher in the fusion-positive group, while *CDKN2A* loss tended to be lower, and both were significantly different in cases analyzed exclusively using FoundationOne CDx (Table S5). The high frequency of *TERT* promoter mutations and the low frequency of *TP53* mutations in the fusion-positive group were also consistent with previous reports [1, 23] (Table 3, Table S6). *CDK4* and *MDM2* amplification may contribute to the activation of the Rb and TP53 pathways as secondary drivers, in addition to the RTK/RAS/PI3K pathway. There was no significant difference in amplification of *MET* and *PDGFRA* between the two groups; however, one case of *PDGFRA* amplification was observed in the fusion-positive group (an *F3T3* fusion-positive case), suggesting that *PDGFRA* amplification and *F3T3* fusion are not strictly mutually exclusive. This finding is consistent with the report by Mata et al. [23]. It is also noteworthy that there was a mutually exclusive relationship with genes encoding receptor tyrosine kinase protein domains, such as *KIT* and *KDR*. *CDK4* and *MDM2* amplification may therefore act as secondary drivers, contributing to the activation of the Rb and TP53 pathways alongside the RTK/RAS/PI3K pathway.

An interesting finding of this study was the high frequency of *FGFR3* amplification in the *FGFR*::*TACC* fusion-positive group. Mata et al. reported that *FGFR3* amplification was observed in approximately 30% (11/37 cases) of GBM, IDH-wt cases harboring the *F3T3* fusion [23]. Other cancer cohort studies have also found *FGFR3* amplification in approximately 10 to 30% of non-small cell lung cancer and bladder cancer cases harboring *F3T3* fusions [36, 37]. Parker et al. demonstrated that the *F3T3* fusion is generated by a tandem duplication of approximately 70 kb at 4p16.3, which may contribute to focal copy number gain at the *F3T3* locus [7]. Consistent with this, Frattini et al. reported the occurrence of *EGFR*::*SEPT14* and *EGFR*::*PSPH* fusions occurring within amplified *EGFR* regions, supporting the idea that *F3T3* fusions may also be associated with co-alterations at the same RTK locus [38]. Taken together, these findings suggest that dual *FGFR3*-activating events—*F3T3* fusion together with *FGFR3* amplification—may synergistically enhance downstream signaling.

Regarding treatment, erdafitinib, administered in the tumor-agnostic RAGNAR trial, and fexagratinib, administered to *FGFR* fusion-positive gliomas in the TARGET trial, are both tyrosine kinase inhibitors that suppress activation of the FGFR tyrosine kinase domain driven by activating point mutations or fusions [28, 29]. The expression level of *FGFR3* in tumors harboring both *F3T3* fusion and *FGFR3* amplification remains unknown and warrants further investigation.

4.2 | *FGFR1* Mutation in GBM, IDH-wt

The most frequent *FGFR1* variants in central nervous system tumors are N546 and K656 mutations, commonly referred to as *FGFR1* hotspot mutations [39]. Recently, *FGFR1* hotspot mutations have also been identified in approximately 10%–21% of patients with DMGs [40–43]. In a review by Vuong et al., *FGFR1* hotspot mutations were identified as favorable prognostic factors in DMGs [44]. However, the prevalence and genetic features of *FGFR1* mutations in GBM, IDH-wt have not been comprehensively evaluated. To our knowledge, this study is the first to specifically investigate *FGFR1* mutations and their associated molecular pathological characteristics in GBM, IDH-wt.

13497006, 0, Downloaded from https://onlinelibrary.wiley.com/doi/10.1111/cas.70347 by Okayama University, Wiley Online Library on [13/03/2026]. See the Terms and Conditions (https://onlinelibrary.wiley.com/terms-and-conditions) on Wiley Online Library for rules of use; OA articles are governed by the applicable Creative Commons License

In our study, 31 patients (2.8%) with GBM, IDH-wt harbored *FGFR1* mutations. Among these patients, an almost mutually exclusive relationship with *EGFR* and *PDGFRA* alterations was observed, both of which were significantly more frequent in the mutation-negative group. These findings may reflect differences in driver genes. Furthermore, *CDKN2A/2B* loss tended to be less frequent in the mutation-positive group. With respect to SNVs, *ATRX* and *NF1* mutations were significantly more common in the mutation-positive group. Schellur et al. reported that *ATRX* and *NF1* mutations were significantly associated with DMGs harboring *FGFR1* mutations, and a similar trend was observed in GBM, IDH-wt [41]. Conversely, *TERT* and *PTEN* mutations were significantly less common, which represents a novel finding. *TERT* promoter and *ATRX* mutations are frequent in gliomas, and mutations in both genes are associated with enhanced telomere maintenance; however, they are known to be almost mutually exclusive [45, 46]. Killela et al. and Eckel-Passow et al. showed that *TERT* promoter mutations tend to coexist with typical adult glioma features, whereas *ATRX* mutations are common in *IDH*-mutant and pediatric gliomas and are closely associated with alternative lengthening of telomeres (ALT) [45, 46]. Our findings suggest that these tumors rely on an ALT-like telomere maintenance program rather than on canonical, *TERT* promoter-driven telomerase activation. Generally, GBM, IDH-wt with *TERT* promoter mutations is considered to have a poor prognosis, while those with the *ATRX* mutation are thought to have a relatively favorable prognosis [45]. Based on the genetic profile observed in this study, GBM, IDH-wt with *FGFR1* mutations may possess molecular features associated with a favorable prognosis, as previously reported in DMGs. However, our study did not demonstrate a survival advantage. Further investigation into the relationship between *FGFR1* mutations and genetic alterations involved in telomerase maintenance is warranted.

FGFR1 mutation-positive tumors exhibited significantly higher TMB compared with mutation-negative tumors. Although our study did not evaluate responses to immune checkpoint inhibitors (ICIs), elevated TMB is generally associated with increased neoantigen load and potential responsiveness to ICIs in other tumor types [47, 48]. Therefore, prospective studies assessing the efficacy of ICIs in *FGFR1*-mutated GBM—particularly in combination with *FGFR* inhibitors—are warranted.

Verhaak et al. and Neftel et al. identified *NF1* mutations as a defining feature of the mesenchymal GBM subtype [49, 50]. Furthermore, Marques et al. reported that *NF1* mutations in GBM are associated with aberrant RAF/MEK activation [51]. The high frequency of *NF1* mutations and elevated TMB in the *FGFR1*-mutant subgroup in this study suggests that these tumors constitute a genetically complex, MAPK-driven subset within GBM, IDH-wt. Taken together, these findings indicate that GBM, IDH-wt with *FGFR1* mutations is characterized by ATRX-related telomere maintenance, activation of the NF1/MAPK pathway, and frequent co-mutations in epigenetic and PI3K pathway genes, which may be distinct from the "canonical" GBM, IDH-wt profile (e.g., *EGFR* amplification and *TERT* promoter mutation).

As a limitation, CGP in Japan is approved only for patients who have exhausted standard treatments, which may introduce selection bias due to left truncation and underrepresent patients with very poor prognosis [33]. Missing clinical variables, such as OS, as well as the absence of imaging findings and tumor location data, may limit the precision of survival analyses and clinical characterization. In addition, treatment details were incompletely recorded in the C-CAT database, and treatment strategies—including clinical trial enrollment—may have differed between groups.

Furthermore, the definition of CNAs varies across CGP platforms. For example, FoundationOne CDx defines amplification as a copy number of ≥ 6 in tumors with a purity of $\geq 20\%$; GenMineTOP defines amplification as a copy number of ≥ 6; and the OncoGuide NCC Oncopanel defines amplification as a median depth of ≥ 200 and a copy number of ≥ 8 ($\log_2$ depth ratio ≥ 2). GenMineTOP, a dual DNA/RNA panel, has been reported to have a higher gene fusion detection rate than other platforms [52]; however, it does not report *CDKN2A/2B* or *PTEN* loss. When comparing detection rates between FoundationOne CDx and GenMineTOP, the latter showed significantly lower detection rates for *SOX2* and *HGF* amplification, as well as for SNVs in *NOTCH1/3*, *PIK3CA*, *KMT2D*, *SPEN*, *ATRX*, and *FGFR3* (Table S7).

There were no significant differences in the distribution of CGP platforms between the *FGFR*::*TACC* fusion-positive and -negative groups or between the *FGFR1* mutation-positive and -negative groups. Nonetheless, because multiple panels were used, residual confounding due to platform-specific differences in gene coverage and analytical sensitivity cannot be excluded.

In conclusion, this largest cohort of *FGFR* alterations in GBM, IDH-wt revealed differential genetic profiles compared to the wildtype counterpart, suggesting that GBM, IDH-wt with *FGFR* gene family alterations may constitute a distinct molecular subtype.

Author Contributions

Yasuhito Kegoya: conceptualization, data curation, formal analysis, investigation, methodology, writing – original draft. **Yoshihiro Otani:** conceptualization, data curation, formal analysis, investigation, methodology, writing – original draft. **Ryo Mizuta:** formal analysis, writing – review and editing. **Ryosuke Ikemachi:** formal analysis, writing – review and editing. **Mako Kamiura:** formal analysis, writing – review and editing. **Joji Ishida:** writing – review and editing. **Shinichi Toyooka:** writing – review and editing. **Daisuke Ennishi:** writing – review and editing. **Shuta Tomida:** data curation, writing – review and editing. **Shota Tanaka:** formal analysis, writing – review and editing.

Ethics Statement

Approval of the research protocol in this study was granted by the Institutional Review Board of Okayama University Hospital (2111-047).

Consent

All patients provided written informed consent for the research use of C-CAT data at the timing of CGP testing.

Conflicts of Interest

Shinichi Toyooka received grants or contracts from Eli Lilly and Chugai Pharmaceutical Co. Ltd., and payment or honoraria from Chugai

13497006, 0, Downloaded from https://onlinelibrary.wiley.com/doi/10.1111/cas.70347 by Okayama University, Wiley Online Library on [13/03/2026]. See the Terms and Conditions (https://onlinelibrary.wiley.com/terms-and-conditions) on Wiley Online Library for rules of use; OA articles are governed by the applicable Creative Commons License

Pharmaceutical Co. Ltd. Diasuke Ennishi received grants or contracts from Nippon Shinyaku Co. Ltd., Chugai Pharmaceutical Co. Ltd., Eisai Co. Ltd., and Insight Co. Ltd., and payment or honoraria from Eisai Co. Ltd., Kyowa Kirin Pharmaceutical Co. Ltd., Chugai Pharmaceutical Co. Ltd., AbbVie GK, Bristol Myers Squibb, Nippon Shinyaku Co. Ltd., Ono Pharmaceutical Co. Ltd., and Genmab A/S. Shota Tanaka received grants or contracts from Novocure and Momotaro-Gene, and payment or honoraria from Eisai Co. Ltd. and Daiichi-Sankyo. All other authors report no conflicts of interest.

References

1. T. A. Bale, "FGFR-Gene Family Alterations in Low-Grade Neuroepithelial Tumors," *Acta Neuropathologica Communications* 8 (2020): 21.

2. L. H. Gallo, K. N. Nelson, A. N. Meyer, and D. J. Donoghue, "Functions of Fibroblast Growth Factor Receptors in Cancer Defined by Novel Translocations and Mutations," *Cytokine & Growth Factor Reviews* 26 (2015): 425–449.

3. M. Touat, E. Ileana, S. Postel-Vinay, F. André, and J. C. Soria, "Targeting FGFR Signaling in Cancer," *Clinical Cancer Research* 21 (2015): 2684–2694.

4. D. Singh, J. M. Chan, P. Zoppoli, et al., "Transforming Fusions of FGFR and TACC Genes in Human Glioblastoma," *Science* 337 (2012): 1231–1235.

5. V. Frattini, S. M. Pagnotta, Tala, et al., "A Metabolic Function of FGFR3-TACC3 Gene Fusions in Cancer," *Nature* 553 (2018): 222–227.

6. A. Lasorella, M. Sanson, and A. Iavarone, "FGFR-TACC Gene Fusions in Human Glioma," *Neuro-Oncology* 19 (2017): 475–483.

7. B. C. Parker, M. J. Annala, D. E. Cogdell, et al., "The Tumorigenic FGFR3-TACC3 Gene Fusion Escapes miR-99a Regulation in Glioblastoma," *Journal of Clinical Investigation* 123 (2013): 855–865.

8. S. Sarkar, E. L. Ryan, and S. J. Royle, "FGFR3-TACC3 Cancer Gene Fusions Cause Mitotic Defects by Removal of Endogenous TACC3 From the Mitotic Spindle," *Open Biology* 7 (2017): 170080.

9. L. Y. Ballester, M. Penas-Prado, N. E. Leeds, J. T. Huse, and G. N. Fuller, "FGFR1 Tyrosine Kinase Domain Duplication in Pilocytic Astrocytoma With Anaplasia," *Cold Spring Harbor Molecular Case Studies* 4 (2018): a002378.

10. D. T. W. Jones, B. Hutter, N. Jäger, et al., "Recurrent Somatic Alterations of FGFR1 and NTRK2 in Pilocytic Astrocytoma," *Nature Genetics* 45 (2013): 927–932.

11. J. Zhang, G. Wu, C. P. Miller, et al., "Whole-Genome Sequencing Identifies Genetic Alterations in Pediatric Low-Grade Gliomas," *Nature Genetics* 45 (2013): 602–612.

12. T. Kohno, M. Kato, S. Kohsaka, et al., "C-CAT: The National Datacenter for Cancer Genomic Medicine in Japan," *Cancer Discovery* 12 (2022): 2509–2515.

13. Y. Mukai and H. Ueno, "Establishment and Implementation of Cancer Genomic Medicine in Japan," *Cancer Science* 112 (2021): 970–977.

14. R. Kundra, H. Zhang, R. Sheridan, et al., "OncoTree: A Cancer Classification System for Precision Oncology," *JCO Clinical Cancer Informatics* 5 (2021): 221–230.

15. WHO Classification of Tumours Editorial Board, *World Health Organization Classification of Tumours of the Central Nervous System*, 5th ed. (International Agency for Research on Cancer, 2021).

16. Z. S. Bao, H. M. Chen, M. Y. Yang, et al., "RNA-Seq of 272 Gliomas Revealed a Novel, Recurrent PTPRZ1-MET Fusion Transcript in Secondary Glioblastomas," *Genome Research* 24 (2014): 1765–1773.

17. K. Yoshihara, Q. Wang, W. Torres-Garcia, et al., "The Landscape and Therapeutic Relevance of Cancer-Associated Transcript Fusions," *Oncogene* 34 (2015): 4845–4854.

18. A. L. Di Stefano, A. Fucci, V. Frattini, et al., "Detection, Characterization, and Inhibition of FGFR-TACC Fusions in IDH Wild-Type Glioma," *Clinical Cancer Research* 21 (2015): 3307–3317.

19. S. D. Ferguson, S. Zhou, J. T. Huse, et al., "Targetable Gene Fusions Associate With the IDH Wild-Type Astrocytic Lineage in Adult Gliomas," *Journal of Neuropathology and Experimental Neurology* 77 (2018): 437–442.

20. K. Na, H. S. Kim, H. S. Shim, J. H. Chang, S. G. Kang, and S. H. Kim, "Targeted Next-Generation Sequencing Panel (TruSight Tumor 170) in Diffuse Glioma: A Single Institutional Experience of 135 Cases," *Journal of Neuro-Oncology* 142 (2019): 445–454.

21. S. Asif, R. Fatima, R. Krc, J. Bennett, and S. Raza, "Comparative Proteogenomic Characterization of Glioblastoma," *CNS Oncology* 8 (2019): CNS37.

22. D. S. Nørøxe, C. W. Yde, O. Østrup, et al., "Genomic Profiling of Newly Diagnosed Glioblastoma Patients and Its Potential for Clinical Utility – A Prospective, Translational Study," *Molecular Oncology* 14 (2020): 2727–2743.

23. D. A. Mata, J. K. Benhamida, A. L. Lin, et al., "Genetic and Epigenetic Landscape of IDH-Wildtype Glioblastomas With FGFR3-TACC3 Fusions," *Acta Neuropathologica Communications* 8 (2020): 186.

24. A. L. Di Stefano, A. Picca, E. Saragoussi, et al., "Clinical, Molecular, and Radiomic Profile of Gliomas With FGFR3-TACC3 Fusions," *Neuro-Oncology* 22 (2020): 1614–1624.

25. J. Schittenhelm, L. Ziegler, J. Sperveslage, et al., "FGFR3 Overexpression Is a Useful Detection Tool for FGFR3 Fusions and Sequence Variations in Glioma," *Neuro-Oncology Practice* 8 (2021): 209–221.

26. A. Dono, H. El Achi, B. E. Bundrant, et al., "Infiltrating Gliomas With FGFR Alterations: Histologic Features, Genetic Alterations, and Potential Clinical Implications," *Cancer Biomarkers* 36 (2023): 117–131.

27. H. Bae, B. Lee, S. Hwang, J. Lee, H. S. Kim, and Y. L. Suh, "Clinicopathological and Molecular Characteristics of *IDH*-Wildtype Glioblastoma With *FGFR3::TACC3* Fusion," *Biomedicine* 12 (2024): 150.

28. S. Pant, M. Schuler, G. Iyer, et al., "Erdafitinib in Patients With Advanced Solid Tumours With FGFR Alterations (RAGNAR): An International, Single-Arm, Phase 2 Study," *Lancet Oncology* 24 (2023): 925–935.

29. A. Picca, A. L. Di Stefano, J. Savatovsky, et al., "TARGET: A Phase I/II Open-Label Multicenter Study to Assess Safety and Efficacy of Fexagratinib in Patients With Relapsed/Refractory FGFR Fusion-Positive Glioma," *Neuro-Oncology Advances* 6 (2024): vdae068.

30. C. G. Duncan, P. J. Killela, C. A. Payne, et al., "Integrated Genomic Analyses Identify ERRFI1 and TACC3 as Glioblastoma-Targeted Genes," *Oncotarget* 1 (2010): 265–277.

31. Z. Wu, O. Lopes Abath Neto, T. A. Bale, et al., "DNA Methylation Analysis of Glioblastomas Harboring FGFR3-TACC3 Fusions Identifies a Methylation Subclass With Better Patient Survival," *Acta Neuropathologica* 144 (2022): 155–157.

32. M. van der Meulen, R. C. Ramos, M. R. Voisin, et al., "Differences in Methylation Profiles Between Long-Term Survivors and Short-Term Survivors of IDH-Wild-Type Glioblastoma," *Neuro-Oncology Advances* 6 (2024): vdae001.

33. T. Tamura, M. Ikegami, Y. Kanemasa, et al., "Selection Bias due to Delayed Comprehensive Genomic Profiling in Japan," *Cancer Science* 114 (2023): 1015–1025.

34. K. J. Granberg, M. Annala, B. Lehtinen, et al., "Strong FGFR3 Staining Is a Marker for FGFR3 Fusions in Diffuse Gliomas," *Neuro-Oncology* 19 (2017): 1206–1216.

35. F. Bielle, A. L. Di Stefano, D. Meyronet, et al., "Diffuse Gliomas With FGFR3-TACC3 Fusion Have Characteristic Histopathological and Molecular Features," *Brain Pathology* 28 (2018): 674–683.

13497006, 0, Downloaded from https://onlinelibrary.wiley.com/doi/10.1111/cas.70347 by Okayama University, Wiley Online Library on [13/03/2026]. See the Terms and Conditions (https://onlinelibrary.wiley.com/terms-and-conditions) on Wiley Online Library for rules of use; OA articles are governed by the applicable Creative Commons License

36. A. H. Nassar, K. Lundgren, M. Pomerantz, et al., "Enrichment of FGFR3-TACC3 Fusions in Patients With Bladder Cancer Who Are Young, Asian, or Have Never Smoked," *JCO Precision Oncology* 2 (2018): PO.18.00013.

37. A. Qin, A. Johnson, J. S. Ross, et al., "Detection of Known and Novel FGFR Fusions in Non-Small Cell Lung Cancer by Comprehensive Genomic Profiling," *Journal of Thoracic Oncology* 14 (2019): 54–62.

38. V. Frattini, V. Trifonov, J. M. Chan, et al., "The Integrated Landscape of Driver Genomic Alterations in Glioblastoma," *Nature Genetics* 45 (2013): 1141–1149.

39. S. Engelhardt, F. Behling, R. Beschorner, et al., "Frequent FGFR1 Hotspot Alterations in Driver-Unknown Low-Grade Glioma and Mixed Neuronal-Glial Tumors," *Journal of Cancer Research and Clinical Oncology* 148 (2022): 857–866.

40. A. Picca, G. Berzero, F. Bielle, et al., "FGFR1 Actionable Mutations, Molecular Specificities, and Outcome of Adult Midline Gliomas," *Neurology* 90 (2018): e2086–e2094.

41. U. Schüller, P. Iglauer, M. M. Dorostkar, et al., "Mutations Within FGFR1 Are Associated With Superior Outcome in a Series of 83 Diffuse Midline Gliomas With H3F3A K27M Mutations," *Acta Neuropathologica* 141 (2021): 323–325.

42. C. Gestrich, K. Grieco, H. G. Lidov, et al., "H3K27-Altered Diffuse Midline Gliomas With MAPK Pathway Alterations: Prognostic and Therapeutic Implications," *Journal of Neuropathology and Experimental Neurology* 83 (2023): 30–35.

43. E. A. Williams, P. K. Brastianos, H. Wakimoto, et al., "A Comprehensive Genomic Study of 390 H3F3A-Mutant Pediatric and Adult Diffuse High-Grade Gliomas, CNS WHO Grade 4," *Acta Neuropathologica* 146 (2023): 515–525.

44. H. G. Vuong, H. T. Le, T. N. M. Ngo, et al., "H3K27M-Mutant Diffuse Midline Gliomas Should Be Further Molecularly Stratified: An Integrated Analysis of 669 Patients," *Journal of Neuro-Oncology* 155 (2021): 225–234.

45. J. E. Eckel-Passow, D. H. Lachance, A. M. Molinaro, et al., "Glioma Groups Based on 1p/19q, IDH, and TERT Promoter Mutations in Tumors," *New England Journal of Medicine* 372 (2015): 2499–2508.

46. P. J. Killela, Z. J. Reitman, Y. Jiao, et al., "TERT Promoter Mutations Occur Frequently in Gliomas and a Subset of Tumors Derived From Cells With Low Rates of Self-Renewal," *Proceedings of the National Academy of Sciences of the United States of America* 110 (2013): 6021–6026.

47. S. J. Klempner, D. Fabrizio, S. Bane, et al., "Tumor Mutational Burden as a Predictive Biomarker for Response to Immune Checkpoint Inhibitors: A Review of Current Evidence," *Oncologist* 25 (2020): e147–e159.

48. D. L. Jardim, A. Goodman, D. de Melo Gagliato, and R. Kurzrock, "The Challenges of Tumor Mutational Burden as an Immunotherapy Biomarker," *Cancer Cell* 39 (2021): 154–173.

49. C. Neftel, J. Laffy, M. G. Filbin, et al., "An Integrative Model of Cellular States, Plasticity, and Genetics for Glioblastoma," *Cell* 178 (2019): 835–849.e821.

50. R. G. Verhaak, K. A. Hoadley, E. Purdom, et al., "Integrated Genomic Analysis Identifies Clinically Relevant Subtypes of Glioblastoma Characterized by Abnormalities in PDGFRA, IDH1, EGFR, and NF1," *Cancer Cell* 17 (2010): 98–110.

51. C. Marques, T. Unterkircher, P. Kroon, et al., "NF1 Regulates Mesenchymal Glioblastoma Plasticity and Aggressiveness Through the AP-1 Transcription Factor FOSL1," *eLife* 10 (2021): 10.

52. K. Watanabe, M. Ogawa, A. Shinozaki-Ushiku, et al., "Real-World Data Analysis of Genomic Alterations Detected by a Dual DNA-RNA Comprehensive Genomic Profiling Test," *Cancer Science* 116 (2025): 1984–1995.

Supporting Information

Additional supporting information can be found online in the Supporting Information section. **Figure S1:** Summary of the clinical and genetic features in patients with *FGFR* gene family alterations, excluding *FGFR*::*TACC* fusion and *FGFR1* mutation in glioblastoma, IDH-wildtype. **Figure S2:** Kaplan–Meier survival curve demonstrating overall survival in patients with glioblastoma, IDH-wildtype harboring *FGFR* gene family alterations. **Figure S3:** Violin plots of (A) tumor mutation burden score, (B) number of gene rearrangements/structural atypia, (C) number of substitutions, insertions, and deletions, (D) number of copy number alterations of genes in glioblastoma, IDH-wildtype with *FGFR*::*TACC* fusion. **Figure S4:** Violin plots of (A) tumor mutation burden score, (B) number of gene rearrangements/structural atypia, (C) number of substitutions, insertions, and deletions, (D) number of copy number alterations of genes in glioblastoma, IDH-wildtype with *FGFR1* mutation. **Figure S5:** Kaplan–Meier survival curve demonstrating overall survival in glioblastoma, IDH-wildtype with *FGFR*::*TACC* fusion and those with gene *FGFR1* mutation. **Table S1:** Evidence levels defined by C-CAT. **Table S2:** Clinical and genetic characteristics of glioblastoma, IDH-wildtype with other *FGFR* gene alterations. **Table S3:** Genes with statistically significant differences between *FGFR*::*TACC* fusion positive and negative groups, and between *FGFR1* mutation positive and negative groups in glioblastoma, IDH-wildtype not listed in the overall mutation frequency ranking (Table 3). **Table S4:** Comparison of clinical and genetic characteristics between *FGFR*::*TACC* fusion and *FGFR1* mutation in glioblastoma, IDH-wildtype. **Table S5:** Comparison of copy number alterations frequencies in *FGFR*::*TACC* fusion and *FGFR1* mutation subgroups of glioblastoma, IDH-wildtype, ordered by overall alterations frequency (comprehensive genome profiling platforms limited to FoundationOne CDx). **Table S6:** Comparison of single nucleotide variant frequencies in *FGFR*::*TACC* fusion and *FGFR1* mutation subgroups of glioblastoma, IDH-wildtype, ordered by overall mutation frequency (comprehensive genome profiling platforms limited to FoundationOne CDx). **Table S7:** Comparison of gene alteration detection rates between major panels (FoundationOneCDx vs. GenMineTOP). GenMineTOP does not provide information on *CDKN2A/2B* or *PTEN* loss, so only gene amplifications and SNVs were compared.

13497006, 0, Downloaded from https://onlinelibrary.wiley.com/doi/10.1111/cas.70347 by Okayama University, Wiley Online Library on [13/03/2026]. See the Terms and Conditions (https://onlinelibrary.wiley.com/terms-and-conditions) on Wiley Online Library for rules of use; OA articles are governed by the applicable Creative Commons License